Plasma Chemistry and Plasma Processing, Vol. 8, No. 3, 1988

Plasma-Assisted Etching of Paper

S. Sapieha,[1] A. M. Wrobel,[2,3] and M. R. Wertheimer[2]

Received October 14, 1987; revised December 5, 1987

The effects of plasma etching on surface structure and chemistry of several papers have been investigated. Plasma etching acts like a fine microtome, continuously removing infinitesimally thin layers at the surface. It has allowed us to observe the internal structure of fibers, and interfiber bonding. The kinetics of plasma etching and its temperature dependence are reported; the thermal activation energy determined from the latter was found to be 0.15 eV. Possible applications of plasma etching techniques to study the structural and physical properites of paper in the z-direction and the distribution of coating material across the thickness of a paper sample are discussed.

KEY WORDS: Microwave plasma; plasma etching; cellulose; coating distribution; ESCA; neutron activation.

1. INTRODUCTION

Modification of the surface structure of organic polymers has become important in various industrial, biomedical, and other technological applications.[1,2] Plasma treatment is one of the most efficient methods for surface modification, affecting such properties as wettability,[1,3] adhesion,[3,4] and friction.[5] A plasma may be roughly defined as a combination of neutral and positively and negatively charged particles, which is electrically neutral on a macroscopic scale. A plasma or glow discharge is initiated when an electron is released by some means (for example, photoionization or field emission) in a gas to which an electric field is applied. The plasma state

[1] Pulp and Paper Research Institute of Canada, 570 St. John's Blvd., Pointe Claire, Québec, H9R 3J9, Canada.

[2] "Groupe des Couches Minces" and Department of Engineering Physics, Ecole Polytechnique, Box 6079, Station "A," Montreal, Quebec, H3C 3A7, Canada.

[3] Permanent address: Center for Molecular and Macromolecular Studies, Polish Academy of Sciences, 90-362 Lodz, Ul. Boczna 5, Poland.

0272-4324/88/0900-0331$06.00/0 © 1988 Plenum Publishing Corporation

can be classified into several categories depending on the means to induce it; one of the forms most widely used in the paper industry is the corona discharge. Goring[6] found that corona treatment leads to a significant improvement in the wet bonding of cellulose strips. Bonding strength of cellulose to synthetic polymers is also improved by corona treatment.[7,8] Suranyi *et al.*[9] used corona treatment in air as a means for the recovery of the wettability of aged corrugated board. However, low-pressure, high-frequency "cold" plasma (or glow discharge), the category discussed exclusively in the present paper, has also been found to give rise to bonding enhancement in cellulosic products.[10]

The surface-limited nature of plasma–solid reactions has been a major advantage in another class of applications of plasmas, namely etching. Plasma (or dry) etching employs a glow discharge to generate active species such as atoms or free radicals from a relatively inert molecular gas. These species diffuse to the substrate where they react with the surface molecules to produce volatile reaction products. Plasma etching has largely replaced wet chemical etching in the electronics industry, for the production of very large scale integrated (VLSI) circuits, printed circuit boards, etc.[11]

Plasma etching and plasma ashing of cellulosic materials have also been used as a means for preparing samples for microscopic studies. The use of an air plasma for electron microscopy studies of cotton and wool was reported by Kassenbeck[12] as early as 1958, followed soon thereafter by numerous others: regenerated cellulose,[13-15] wood[15] and cellulosic fibers.[13,16,17] Dumitrescu *et al.*[18] used a "cold" plasma of argon to etch cotton, wood cellulose, and viscose fibers in order to study their internal morphologies. A review of early applications of plasma etching to cellulosic materials is given by Thomas.[19] Pederson[20] correlated etch characteristics in CF_4/O_2 plasma with the composition of several polymers and found that cellulose shows the highest etch rate (700 nm/min), compared with 130 nm/min for polyimide (Kapton). Generally, the etch rate of a given polymer appears to correlate with its susceptibility to chain scission by high-energy irradiation.[20] This is high for cellulose, while low-etch-rate polymers tend to undergo surface cross-linking instead of scission. Cain *et al.*[21] found that hydrogen abstraction by fluorine leads to enhanced etching of saturated polymer structures while addition of fluorine is the dominant mechanism for unsaturated moieties.

The present paper reports a study on CF_4/O_2 plasma etch kinetics of several types of papers, along with changes in their morphological structure and their chemical composition at the surface after etching. Possible applications of plasma etching to study the *z*-directional structural properties of paper, for example the distribution of coating material across the paper thickness, are discussed.

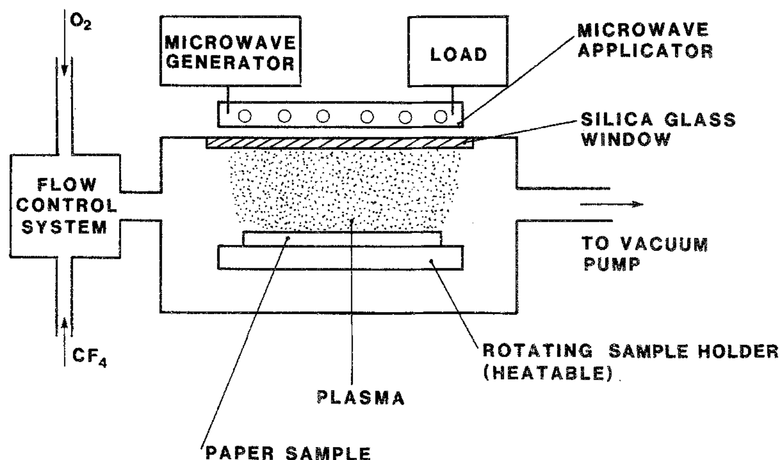

Fig. 1. Schematic diagram of the plasma-etching system.

2. EXPERIMENTAL

2.1. Apparatus

The present plasma etching studies were performed using a "large volume microwave plasma" (LMP) system (Polyplasma Inc., model "LMP 83-3"),[22,23] which is shown schematically in Fig. 1. The plasma is induced in a gas flow at low pressure using microwave power at 2.45 GHz. In order to ensure uniform etching across the entire sample area, the apparatus is equipped with provisions for simultaneous rotational and translational motion of the sample during treatment. In the present work, samples were rotated at 6 rpm during etching. A typical sample diameter was 10 cm.

A mixture of tetrafluoromethane (CF_4) and oxygen (O_2) was used as the etching gas. The etch rate, *r*, under given conditions was determined from the slope of the weight loss vs. etch time plot. In order to study the effects of two principal etch parameters, gas composition and pressure, the concentration of CF_4 was varied between 0 and 100%, and the overall pressure between 150 and 500 mTorr (20 to 66.5 Pa). Many experiments were done with flow rates of 8 and 62 sccm for CF_4 and O_2, respectively, while the pressure was kept constant at 250 mTorr (33.3 Pa). This condition was found to produce a maximum etch rate in Kapton polyimide. Discharge power was selected between 20 and 160 W.

2.2. Materials

Several different papers have been investigated: Whatman filter paper No. 42, standard kraft handsheets, commercial ink jet paper, and capacitor

and insulating papers. Thickness and oven dry basis weight of the paper samples were determined before and after treatment according to TAPPI standard methods T411m44 and T410os68, respectively. Reference samples, placed underneath the treated samples during etching, show a slight decrease in grammage. This may be due to irreversible changes in water sorption properties during exposure to vacuum. However, these changes are small, comparable to the overall experimental error.

2.3. Analytical Methods (X-ray Photoelectron Spectroscopy and Neutron Activation Analysis)

X-ray photoelectron spectra (XPS) of treated samples were measured using a Vacuum Generators Scientific Ltd. "ESCALAB" spectrometer, with a Mg anode as the K_α photon source. Binding energies were referenced to the hydrocarbon (C_{1s}) peak at 285 eV.

Samples of the ink jet paper were irradiated in a "Slowpoke" reactor at Ecole Polytechnique, using a neutron flux of 10^{12} neutrons/s, and counting was subsequently performed for 5 min. Peaks corresponding to several elements (Al, Ca, Na, Mn, Ti, and Cl) in the coating material were analyzed. Atomic concentrations were determined from peak areas.

3. RESULTS AND DISCUSSION

3.1. Effect of Etch Gas Pressure

The effect of CF_4/O_2 mixture pressure, p, on the etch rate, r, at constant flow ratio ($CF_4/O_2 = 0.2$) is presented in Fig. 2. A distinct maximum in r is observed for both grammage and thickness curves at $p = 250$ mTorr. Similar curves have also been observed for plasma etching of various commercial polymers.[23,24] As explained in Refs. 23 and 24, the maximum in r vs. p may be linked with variations of the electron temperature and the concentrations of etch precursors, namely atomic oxygen and atomic fluorine. The shapes of the etch kinetics curves agree well with optical emission spectroscopy data; these revealed a maximum in the emission intensity of atomic oxygen (486 nm) as a function of pressure.[25] Thus, the increase in r for $p < 250$ mTorr (Fig. 2) may be attributed to a rise in the production rate of atomic oxygen. The drop in r for $p > 250$ mTorr may be related to such factors as a decrease in the population of energetic electrons (which results in decreased rates of production of oxygen and fluorine atoms), increased collisional quenching of excited species, and an increased rate of recombination of oxygen and fluorine atoms.

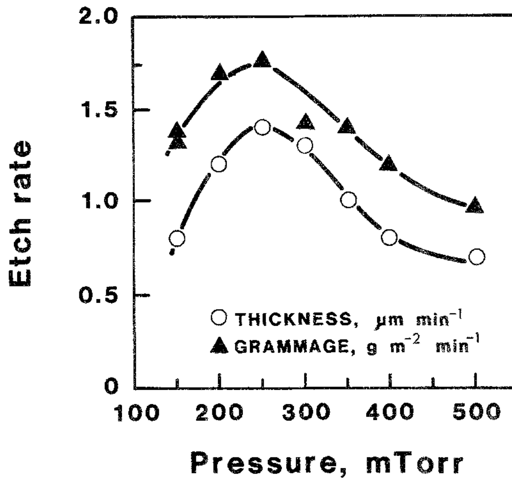

Fig. 2. Etch rate of kraft paper as a function of gas pressure. Flow rate of CF_4 is 20% in O_2.

3.2. Effect of Etch Gas Composition

Figure 3 shows r for kraft paper as a function of CF_4 concentration in the CF_4/O_2 mixture, at constant gas pressure ($p = 250$ mTorr). The etch rate r is seen to increase with increasing concentration of CF_4, reaching a maximum value at about 20%. This is consistent with the optical emission

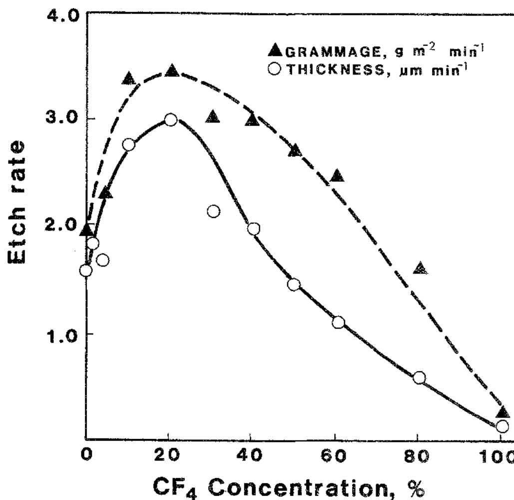

Fig. 3. Etch rate of kraft paper as a function of the percentage (by flow rate) of tetrafluoromethane in oxygen. Total gas pressure was 250 mTorr.

spectroscopy results for CF_4/O_2 plasma etching of polyimide[24,26]; the emission intensity of atomic oxygen was found to increase sharply to a maximum with the corresponding increase in CF_4 concentration.

Halogenated (particularly fluorine-bearing) compounds may be considered to play a catalytic role in plasma etching of organic materials. Fluorine atoms produced via dissociation of CF_4 can abstract hydrogen atoms from the organic material, producing radical sites according to the following reaction scheme[27]:

$$P + F \rightarrow P^{\cdot} + HF\uparrow \qquad (1)$$

where *P* represents an organic macromolecule. Radical sites can also be formed, however, to a lesser extent, by direct attack of oxygen atoms:

$$P + O \rightarrow P^{\cdot} + OH \qquad (2)$$

The resulting radical sites can readily undergo a variety of reactions with oxygen and fluorine atoms:

$$P^{\cdot} + O \rightarrow P'O + CO\uparrow,\ CO_2\uparrow \qquad (3)$$

$$P^{\cdot} + F \rightarrow PF,\ PF_2 \qquad (4)$$

$$PF_2 + F \rightarrow P'F_2 + CF_4\uparrow \qquad (5)$$

$$P'O + F \rightarrow P'OF \qquad (6)$$

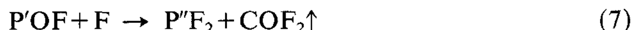

$$P'OF + F \rightarrow P''F_2 + COF_2\uparrow \qquad (7)$$

Reactions (1)-(3) are favored in the low CF_4 concentration range, accounting for the increase in *r* at CF_4 concentration $\leq 20\%$ (Fig. 3). Reactions (4)-(7) are favored at high CF_4 concentrations, and they result in passivation via formation of a fluorinated surface layer which inhibits attack by oxygen atoms. These reactions may also contribute to the observed drop in *r* at concentrations of $CF_4 > 20\%$: In the case of plasma etching of polyimide, an intense fluorination was indeed found to occur for CF_4 concentration $>20\%$, $-CF_2-$ groups being the dominating structural units in the surface layer.[26]

The types of reactions above are confirmed in the present studies of cellulose surfaces using XPS. Figure 4 gives comparisons of survey scans for kraft paper (untreated, curve A), treated with CF_4 (curve B), and treated with a mixture of CF_4/O_2 (20% CF_4, curve C). Plasma etching is seen to result in a significant increase in the oxygen/carbon ratio for sample (C) but no trace of fluorine is noted. If, however, the cellulose is subjected to CF_4 plasma alone, then a new fluorine F_{IS} peak appears. A detailed study of the surface chemistry of plasma-etched cellulose will be published elsewhere.[28]

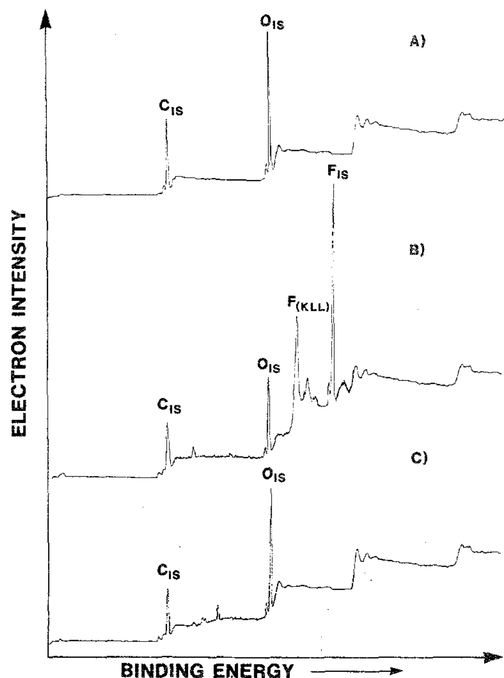

Fig. 4. XPS survey spectra of kraft paper, (a) before and (b) after etching with CF_4; (c) after etching with CF_4/O_2.

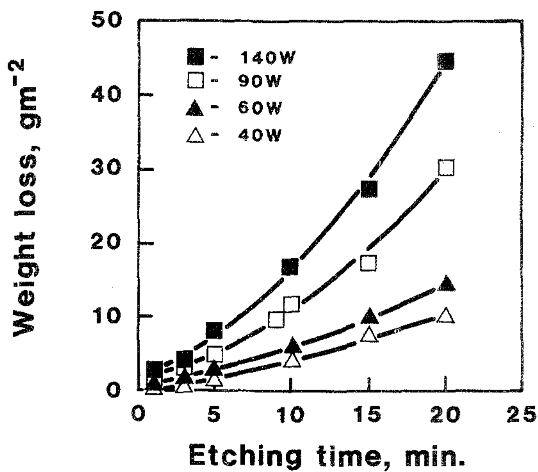

Fig. 5. Weight loss of kraft paper vs. etching time. Flow rate: oxygen, 62 sccm; tetrafluoromethane, 8 sccm. Gas pressure 250 mTorr.

Figure 5 shows typical plots of weight loss of kraft paper versus etching time for different discharge power values. Weight and thickness loss of Whatman filter paper as a function of etching time is presented in Fig. 6. In an ideal case (i.e., constant experimental conditions) the weight loss might be expected to be a linear function of the etching time. The present experimental data, however, show that the etch rate r (proportional to the slope) changes during the experiments. This is similar to observations reported by Pederson[20] for a variety of polymers, and to our own microwave etch studies of Kapton polyimide.[23] This effect is attributable to a rise in the sample temperature resulting from dielectric heating by the high-frequency electric field, possibly combined with inductive heating of the metallic substrate. As the etch rate r is thermally activated, it can be expressed by an Arrhenius equation as follows:

$$r = r_0 \exp(-E/kT) \tag{8}$$

where r_0 is the prefactor (temperature-independent etch rate coefficient), E is the thermal activation energy, k is the Boltzmann's constant, and T is the absolute temperature. The temperature increase during etching is therefore responsible for the time-dependent etch rates as observed in Figs. 5 and 6. This is a desirable effect in commercial applications of plasma etching, as it leads to higher etch rates. However, for the purpose of this work, in order to ensure that thermal decomposition of cellulose does not take place, the range of discharge power was limited. Figure 7 presents the logarithm of etch rate plotted as a function of reciprocal temperature of the sample;

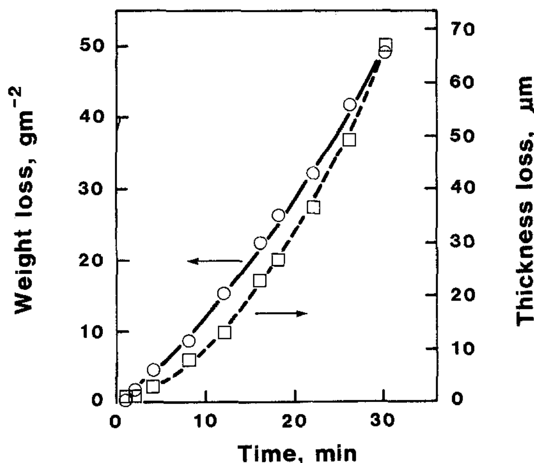

Fig. 6. Weight loss of Whatman filter paper vs. etching time. Flow rate; oxygen, 62 sccm; tetrafluoromethane, 8 sccm. Gas pressure 250 mTorr. Discharge power 90 W.

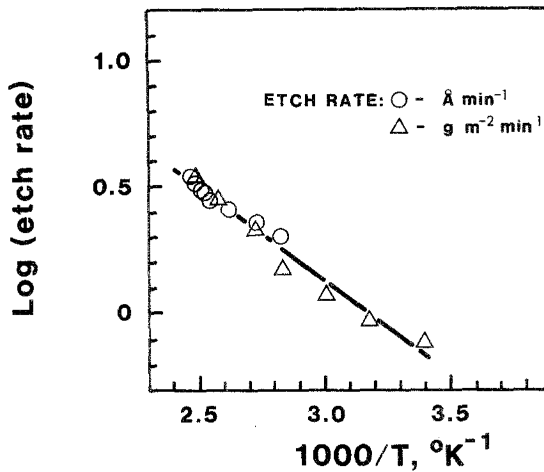

Fig. 7. Arrhenius plot of the etch rate of kraft paper. Circles correspond to data from Pederson.[20] Discharge power 140 W; other conditions as in Fig. 5.

the thermal activation energy calculated using Eq. (8) is found to be $E = 0.15$ eV.

Table I gives the measured etch rates for several papers investigated. For uncoated papers, the etch rate (expressed in thickness per unit time) is seen to be inversely proportional to the density. The grammage and thickness loss curves potentially contain a wealth of information on such physical properties of paper as gravimetric density distribution across the sample thickness, for example. We intend to study this aspect after optimizing the experimental conditions, i.e., limiting the plasma penetration into the paper structure.

Typical SEM micrographs of unetched and plasma-etched kraft and Whatman No. 42 filter papers are presented in Figs. 8 and 9, respectively.

Table I. Apparent Etch Rates of Different Papers (Discharge Power 130 W, Pressure 250 mTorr, Temperature 22°C, Flow 11.4% CF_4 in O_2, Total Gas Flow Rate 70 sccm)

	Thickness	Density	Etch rate	
	(μm)	(g cm^{-3})	(μm min^{-1})	(g m^{-2} min^{-1})
Kraft paper	93	0.46	2.0	2.7
Insulating paper	225	0.8	1.7	N.D.[a]
Capacitor paper	12.7	1.2	1.3	N.D.
Ink jet paper (coated)	112	0.63	0.83	1.2

[a] N.D.—not determined.

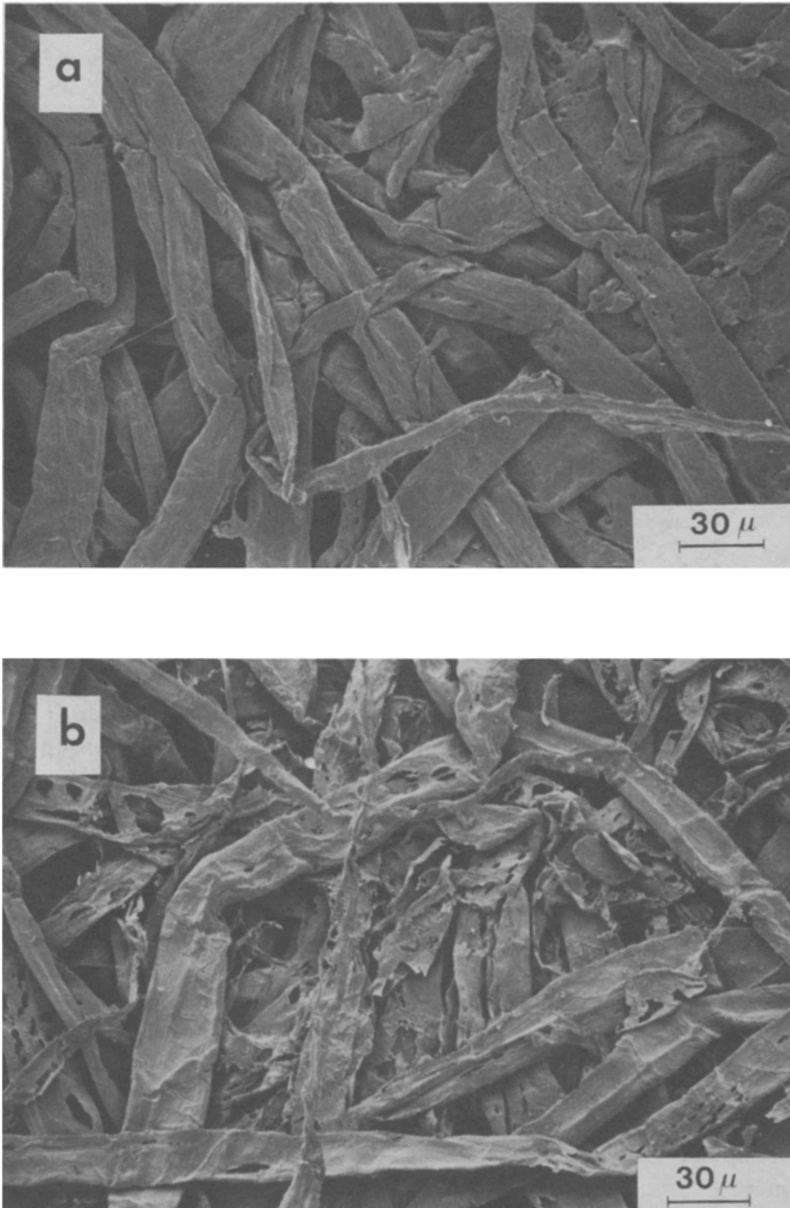

Fig. 8. SEM micrographs of etched kraft paper: (a) before etching; (b) after etching. Power 40 W. Gas pressure 230 mTorr. Etching time 20 min.

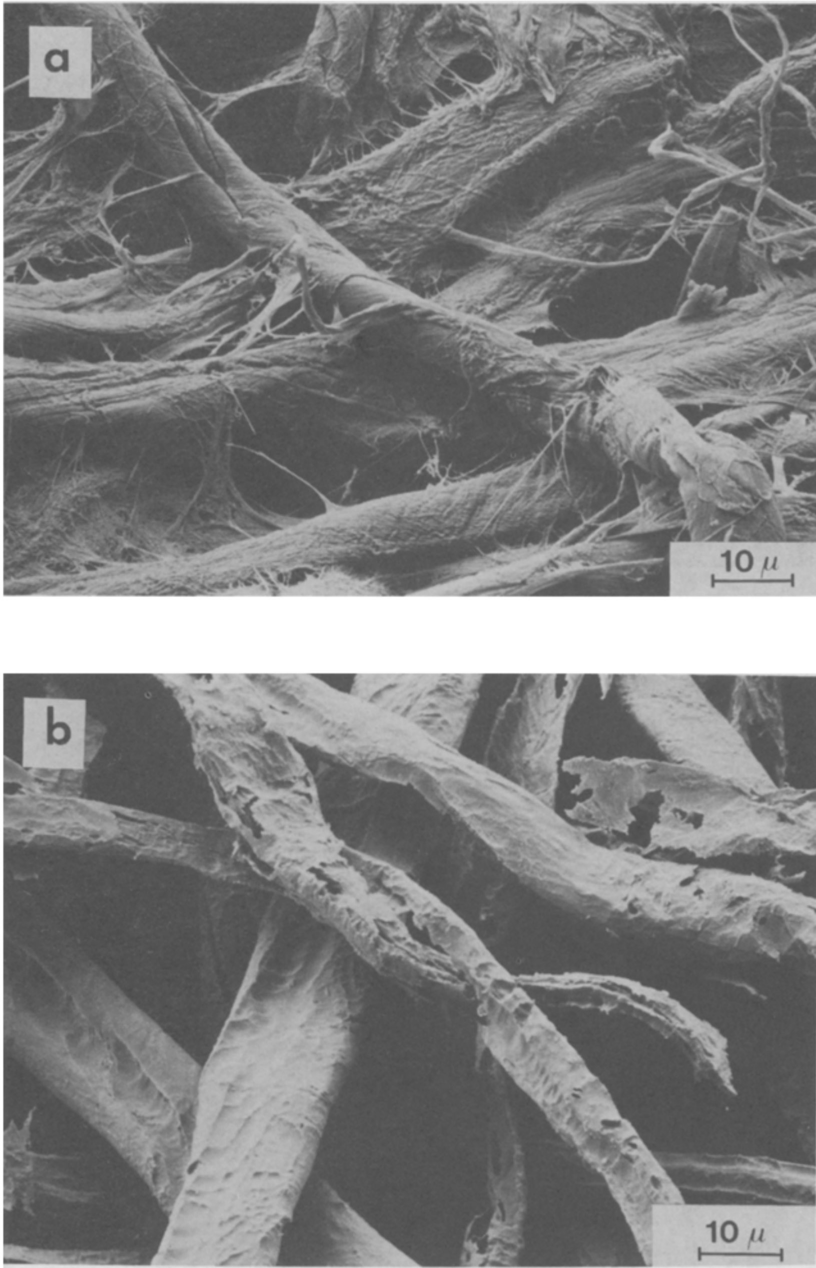

Fig. 9. SEM micrographs of Whatman filter paper: (a) before etching; (b) after etching. Etch conditions as in Fig. 8.

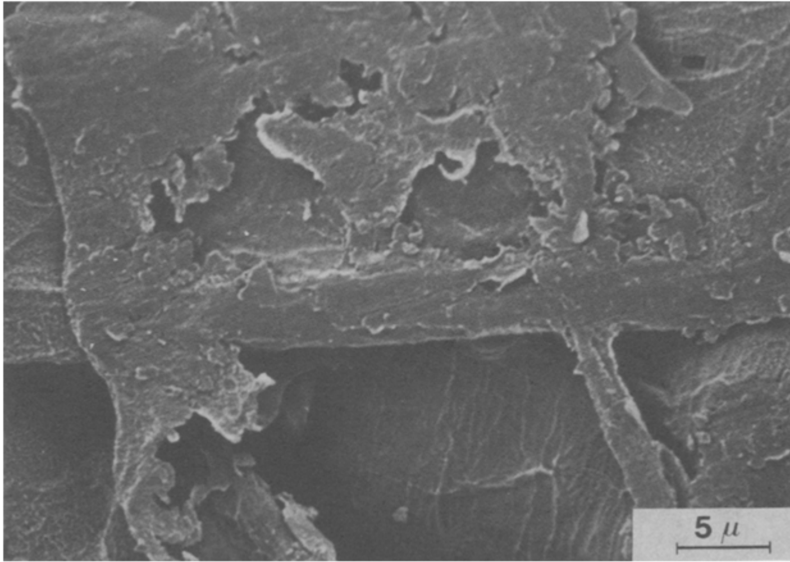

Fig. 10. SEM micrograph of the etched bonded area between two kraft fibers.

Figure 9 shows that the plasma preferentially etches away microfibrils as well as small cellulose fragments and debris. The micrographs suggest that the plasma etch front penetrates to a depth of at least two fiber thicknesses. Such behavior, of course, differs from that observed for polymeric films, where the etch front progresses more or less uniformly across the sample thickness, usually leading only to a microroughening of the polymer surface. However, the complex morphological structure of paper, characterized by surface and bulk porosity and nonuniform mass density distribution across the sample thickness, affects the distribution of plasma and thus the etching front. Microroughening of cellulosic fibers, similar to that observed for conventional polymer films, can also be observed (see, for example, Fig. 8b and 12b).

Figure 10 shows a micrograph of two crossed softwood kraft fibers after etching. The plasma has etched away the top fiber, uncovering the interfiber bonding area and revealing voids between fibers and the bonded areas as well.

3.3. Distribution of Coating Material

Several experimental techniques like grinding[29-31] or microtome sectioning[32,33] have been used to analyze the distribution of coating

material across the thickness of paper samples. A common problem with grinding techniques is the effective removal of the generated dust particles before the sample can be examined.

Plasma etching appears to be well suited for this purpose, as it acts like a fine microtome in continuously removing infinitesimally thin layers of coated paper. The etch rate can be adjusted by a proper selection of etchant gases, their partial pressure, substrate temperature, and discharge power, as outlined in Sections 3.1 and 3.2. The remaining paper sample can then be analyzed for characteristic fillers using several available analytical techniques like ash analysis, ion chromatography, neutron activation, etc.

In the present work, an attempt to study the distribution of coating material in commercial ink jet paper has been made. For this material, the plot of weight loss vs. time was linear under the "standard" etch conditions (12% CF_4 in O_2, $F = 70$ sccm, $P = 130$ W, $p = 200$ mTorr), the slope being $1.2\ g\ m^{-2}\ min^{-1}$. Figure 11 gives the normalized grammage of some elements found in the coating composition as a function of remaining grammage of paper; whereas the concentration of chlorine is seen to vary, the concentrations of other elements (aluminum, calcium, and sodium) change only slightly with the remaining grammage of paper and practically follow the same curve (only aluminum is plotted). These rather interesting results suggest that the filler particles were not removed from the paper during etching, which can be explained by the fact that many inorganic materials do not form volatile compounds in a CF_4/O_2 plasma. Moreover, electrostatic phenomena operating in a plasma, especially in the plasma sheath, may

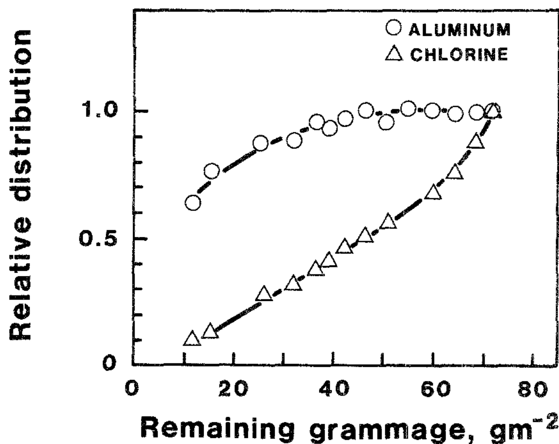

Fig. 11. Distribution of coating composition in ink jet paper as a function of remaining grammage. Data pertaining to only two of the elements analyzed (Cl and Al) are presented.

cause the inorganic filler particles to become charged and to adhere to the substrate. Such particles form a loose dust which can be removed by vacuuming.

XPS survey spectra indicate that plasma etching of coated papers (either in argon or CF_4/O_2 mixture) results in higher-intensity peaks for the filler material, compared to those in a virgin sample. This may result from the fact that in a virgin sample the filler particles are partially coated with the organic binder, which is removed by etching.

3.4. Distribution of Pigment in Lumen-Loaded Fibers

An interesting application of plasma etching, namely to study the pigment distribution inside lumen-loaded fibers, is presented in Fig. 12. Samples were etched at a low rate, so that only the topmost fibers were opened. Micrograph 12a shows the top surface of etched paper at low magnification; large fragments of the fiber wall are seen to have been removed, allowing one to observe the lumen interior. Figure 12b, a higher magnification of a fiber, shows the distribution of TiO_2 particles inside.

4. CONCLUSION

It has been demonstrated that plasma etching acts like a fine microtome in continuously removing infinitesimally thin layers of cellulose. The etch rate of cellulose, a function of experimental conditions such as etch gas pressure, composition, and discharge power, can readily be controlled. Plasma etching may become a useful tool to study the z-directional properties of paper if the penetration of the plasma front into the paper structure is controlled.

ACKNOWLEDGMENTS

The authors wish to thank Dr. Greg Kennedy for the neutron activation analysis, and Mrs. J. Klemberg for ESCA experiments; Miss G. de Silveira of the Pulp and Paper Research Institute of Canada is thanked for performing the scanning electron microscopy. We are grateful to Dr. A. M. Scallan for providing the samples of lumen-loaded fibers. This work was supported in part by the Natural Sciences and Engineering Research Council of Canada (via Coop Grant No. CRD 8457 and personal operating grants to S.S. and M.R.W.), and by the Fonds "Formation de Chercheurs et Aide à la Recherche" (FCAR) of Quebec.

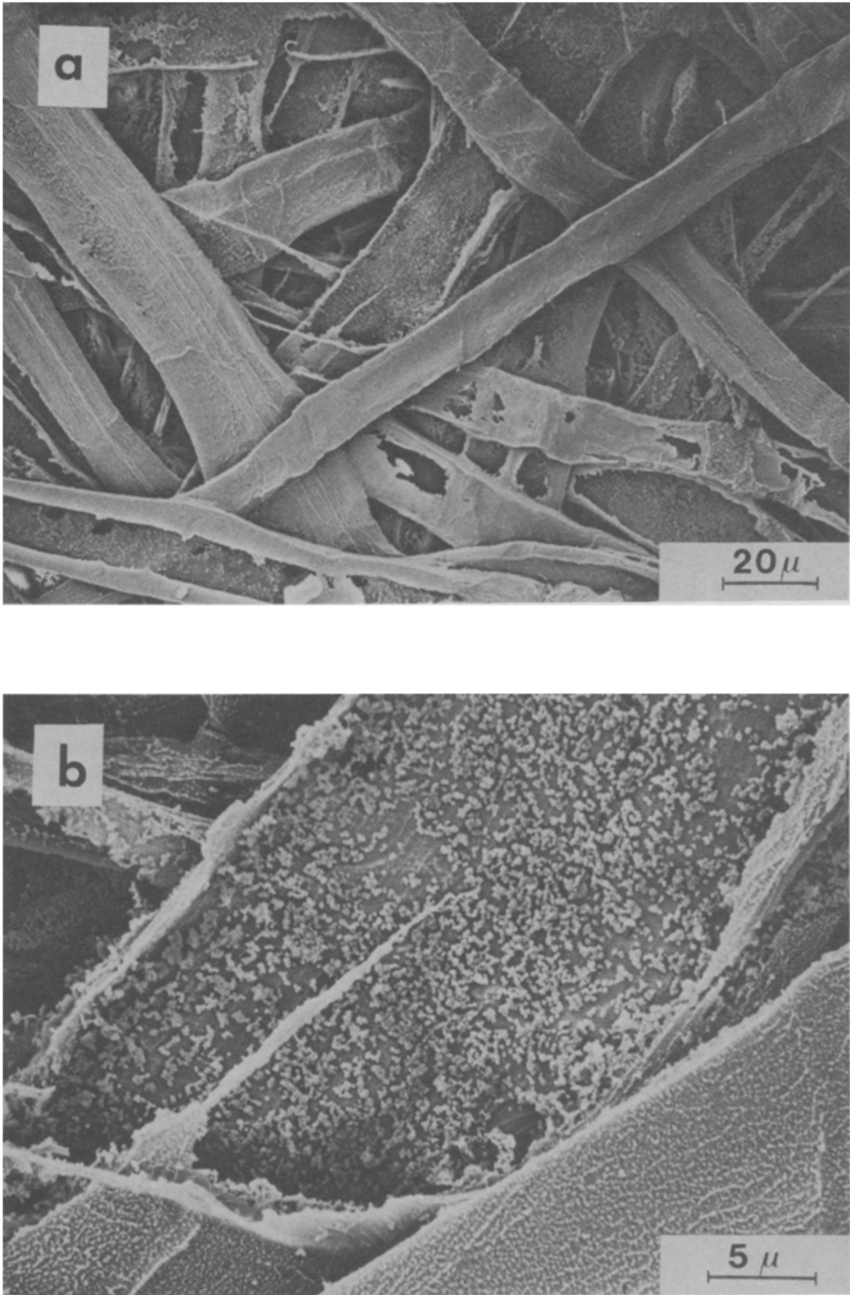

Fig. 12. SEM micrographs of lumen-loaded fibers after plasma-etching, showing TiO_2 particles inside the lumen.

REFERENCES

1. D. T. Clark and W. J. Feast, *Polymer Surfaces*, Wiley, New York (1978).
2. M. R. Wertheimer, J. E. Klemberg-Sapieha, and H. P. Schreiber, *Thin Solid Films* **115**, 109 (1984).
3. S. Wu, *Polymer Interface and Adhesion*, Marcel Dekker, New York (1982).
4. C. Y. Kim, J. Evans, and D. A. I. Goring, *J. Appl. Polym. Sci.* **15**, 1365 (1971).
5. W. J. Thoresen, *Text. Res. J.* **41**, 331 (1971).
6. D. A. I. Goring, *Pulp Pap. Mag. Can.* **68**, T-372 (1967).
7. R. E. Green, *Tappi* **48**, 80A (1965).
8. D. A. I. Goring and G. Suranyi, *Pulp Pap. Mag. Can.* **70**, T390 (1969).
9. G. Suranyi, D. G. Gray, and D. A. I. Goring, *Tappi* **63**, 153 (1986).
10. M. R. Wertheimer, G. Suranyi, and D. A. I. Goring, *Tappi* **55**, 1707 (1972).
11. *Thin Film Processes*, J. L. Vossen and W. Kern, eds., Academic Press, New York (1978).
12. P. Kassenbeck, *Melliand Textilber* **39**, 55 (1958).
13. B. J. Spit, in *Proceedings of the European Regional Conference on Electron Microscopy*, Delft, 1960,
14. B. J. Spit, *Polymer* **4**, 109 (1963).
15. B. J. Spit, *Faserforsch. Textiltech.* **18**, 161 (1967).
16. J. Ising and B. J. Spit, *Proceedings of the 3rd European Conference on Electron Microscopy*, Vol. A, Publishing House of the Czechoslovak Academy of Science, Prague, p. 407.
17. V. Nikonovich, N. D. Burkhanova, S. A. Leont'eva, and K. U. Usmanov, *Cellul. Chem. Tech.* **1**, 171 (1967).
18. S. Dumitrescu, G. Rozmarin, E. Ioanid, and A. Ioanid, *Cellul. Chem. Technol.* **18**, 125 (1984).
19. S. Thomas, in *Techniques and Applications of Plasma Chemistry*, J. R. Hollahan and A. T. Bell, eds., Wiley-Interscience, New York (1978), Chapter 8.
20. L. A. Pederson, *J. Electrochem. Soc.* **129**, 205 (1982).
21. S. R. Cain, F. D. Egito, and F. Emmi, *J. Vac. Sci. Technol.* **A5**, 1578 (1987).
22. R. G. Bosisio, M. R. Wertheimer, and C. Weissfloch, *J. Phys. E: Sci. Instrum.* **6**, 628 (1973).
23. B. Lamontagne, A. M. Wrobel, G. Jalbert, and M. R. Wertheimer, *J. Phys. D: Appl. Phys.* **20**, 844 (1987).
24. J. Paraszczak, M. Hatzakis, E. Babich, J. Shaw, E. Arthur, B. Grenon, and M. DePaul, *Microcircuit Eng.* **2**, 517 (1984).
25. S. Dzioba, G. Este, and H. M. Naguib, *J. Electrochem. Soc.* **129**, 2537 (1982).
26. F. D. Egito, F. Emmi, R. S. Horwath, and V. Vukanovic, *J. Vac. Sci. Technol. B* **3**, 893 (1985).
27. M. Kogoma and G. Turban, *Plasma Chem. Plasma Process.* **6**, 349 (1986).
28. S. Sapieha, J. Klemberg-Sapieha, E. Sacher, and M. R. Wertheimer, in preparation; also *Bull. Am. Phys. Soc.* **33**, 1227 (1988).
29. N. J. Beckman and E. I. Plucker, *Proceedings of 1973 TAPPI Coating Conference*, p. 87.
30. T. Hattula and P. J. Aschan, *Pap. Puu* **60**, 665 (1978).
31. P. J. Aschan, T. Hattula, and J. Paakko, *Tappi* **63**, 59 (1980).
32. J. Kuusi and A. Lehtinen, *Pulp Pap. Mag. Can.* **71**, T37 (1970).
33. G. Grant, G. S. Clifton, and J. C. Sheppard, *Tappi* **57**, 127 (1974).